Ultrafast Relaxation Dynamics of Perchlorinated Cycloheptatriene in Solution

O. Schalk and A.-N. Unterreiner*

Institut für Physikalische Chemie, Kaiserstr. 12, 76128 Karlsruhe Universität Karlsruhe (TH), Germany

Received: September 21, 2006; In Final Form: February 27, 2007

The photochemistry of perchlorinated cycloheptatriene ($CHTCl_8$) has been studied by means of ultrafast pump−probe, transient anisotropy and continuous UV-irradiation experiments in various solvents as well as by DFT calculations. After UV-excitation to the 1A″-state, two competing reactions occur—a [1,7]-sigmatropic chlorine migration via two ultrafast internal conversions and a [4,5]-electrocyclization forming octachlorobicylo[3.2.0]-hepta-[2,6]-diene. The first reaction has been studied by excitation with a 263 nm femtosecond-laser pulse. Pump−probe experiments reveal a first, solvent-independent time constant, $\tau_1^{CHTCl_8} = 140$ fs, that can be associated with the electronic relaxation of the 2A′−1A″ transition, while a second one, $\tau_2^{CHTCl_8}$, ranges from 0.9 to 1.8 ps depending on the polarity of the solvent. This finding is consistent with a [1,7]-chlorine migration during the 1A′−2A′ transition where the migrating chlorine atom is partly negatively charged. The charge separation has also been confirmed by DFT calculations. Transient anisotropy measurements result in a time zero value of $r(0) = 0.35$ after deconvolution and a decay constant of $\tau_1^a = 120$ fs, which can be explained by vibrational motions of $CHTCl_8$ in the electronically excited states, 1A″ and 2A′. After continuous UV-irradiation of $CHTCl_8$, octachlorobicylo[3.2.0]hepta-[2,6]-diene is primarily formed with a solvent-dependent yield. From these investigations, we suggest a relaxation mechanism for $CHTCl_8$ after photoexcitation that is comparable to cycloheptatriene.

1. Introduction

The elucidation of ultrafast dynamics in small polyenes after photoexcitation is essential in order to better understand systems that are of biological and technical interest.[1] These processes often include chemical reactions like an electrocyclic ring-opening (-closure), cis−trans isomerizations and atom migrations. In general, photoexcitation promotes a molecule to a spectroscopically bright state which often has 1A″, $1B_u$, or $1B_2$ symmetry (for a molecule with C_s, C_{2h}, or C_{2v} symmetry class, respectively). This state couples via a conical intersection to a dark state of 2A′ , $2A_g$, or $2A_1$ symmetry, which is populated in typically less than 300 fs[2] (note that this state is symmetry forbidden only in the case of C_{2h}-symmetry while for C_{2v} and C_s symmetry, the transition is allowed, but has typically a low oscillator strength[3,4]). The photoinduced reaction finally takes place during an internal conversion back to the ground state. The time constant and branching ratio between competing processes are then determined by the potential energy surface (PES) of the dark state, i.e., the temporal evolution of a wavepacket on this surface and the type of the transition. If the latter is a conical intersection or a weakly avoided crossing, the reaction often takes place in less than 1 ps. In recent years, many systems have been studied both experimentally[5−14] and theoretically;[15−19] however many aspects are still not understood in detail.

One example of such a polyene is cycloheptatriene (CHT).[20−25] CHT has C_s-symmetry and a resonant photoexcitation of the ground state ($S_0 \triangleq 1A'$) leads to a population of the second excited state ($S_2 \triangleq 1A''$). The first excited state ($S_1 \triangleq 2A'$) is electronically dark and, therefore, cannot be reached via a one photon process. At the second internal conversion, a [1,7]-hydrogen shift takes place (for a theoretical treatment, see refs 26 and 27). While the first conversion is believed to occur in less than 60 fs, the time constants for the second conversion diverge between 70 fs[21] and 26 ps.[22,23] Calculations of the potential energy surface of the 2A′ state[26] result in an excited-state barrier between 31.4 kJ/mol for CASSCF/6-31G and 15.6 kJ/mol for CASPT2/ANO allowing no clear assignment of the relevant time constant. Therefore, a more detailed mechanistic understanding requires improvements both experimentally and theoretically. Anisotropy experiments, for example, can give additional information on the temporal evolution of the transition dipole moment. Recently, we[28] reported on an anomalous high initial anisotropy of 0.58 for CHT which was interpreted in terms of a quasi-degeneration between the 1A″ and 2A′ states in the Franck−Condon region. After excitation, the anisotropy rapidly decays within 150 ± 20 fs, which is on the order of the population decay and much faster than the corresponding free rotational correlation times for CHT. Consequently, this relaxation time can be considered as a pseudo-rotation of CHT due to the [1,7]-H migration.

Besides this [1,7]-hydrogen shift, CHT is able to undergo a [4,5]-electrocyclic ring closure leading to bicyclo[3.2.0]hepta-2,6-diene (BHD)[29−35] or to norcaradiene which is followed by a rearrangement to toluene.[29] While the latter reaction is supposed to occur in the vibrational hot ground state,[36,37] the former reaction takes place in the 2A′-state. At low pressures, the conversion to toluene has a quantum yield of nearly one which decreases with increasing pressure.[30] In the liquid phase or in low-temperature matrices, toluene is only formed in small amounts due to a fast energy dissipation to surrounding solvent molecules in the electronic ground state.[31,32] Extended irradiation of CHT then leads to BHD as a major final product[31] with a yield of about 90%.[33] In comparison to the [1,7]-hydrogen shift, this reaction is supposed to be at least a factor 500 slower.[34,35]

* Corresponding author. E-mail: andreas.unterreiner@ipc.uka.de.

10.1021/jp066193f CCC: $37.00
Published on Web 04/12/2007

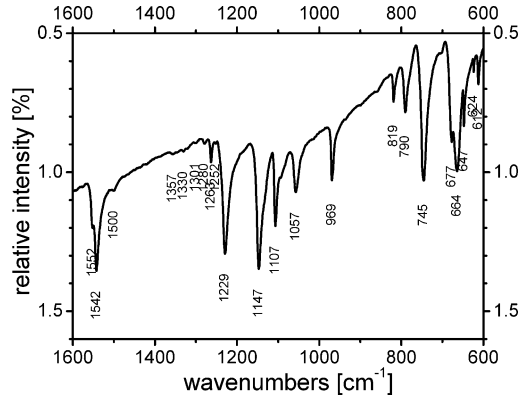

Figure 1. IR spectrum of $CHTCl_8$ in KBr pellets.

Nevertheless, the absolute time constants as well as mechanistic aspects still deserve additional experimental input.

One approach represents the substitution of all H atoms by chlorine atoms in order to study the ultrafast dynamics of the corresponding octachlorocycloheptatriene ($CHTCl_8$). It is expected that a [1,7]-chlorine migration occurs on a longer time scale due to an increased effective mass.[28] Up to now, photochemically induced chlorine migrations in $CHTCl_8$ have not been studied, but there exist several investigations of various thermally allowed pericyclic chlorine shifts.[38−43] The first example of a [1,5]-chlorine shift in a cycloheptatriene analogue was given by Looker[38] who studied 5-chloro-5*H*-dibenzo[*a*,*d*]-cycloheptene. Moreover, he noted that neither 5,5-dichloro-5*H*-benzocycloheptene nor 7,7-dichlorocycloheptatriene gave rearranged chlorides but led to an unknown compound. A similar [1,5]-chlorine migration was identified by van Eis et al.[39] Kessler et al.[40] found by ^1H and ^{13}C NMR spectroscopy that chlorotropylium chloride exists as a mixture of 1,7-, 2,7- and 3,7-dichlorocycloheptatriene and the ionic species. As this finding depends on the polarity of the solvent, it was assumed that the migrating chlorine atom is charged. Furthermore, they found that the barrier of the migration decreases in polar solvents.

To briefly summarize, CHT is a typical example of a small polyene that performs an atom shift during its S_0/S_1-internal conversion. Using ultrafast spectroscopy as well as steady-state illumination of $CHTCl_8$, the effect of perchlorination of polyenes can be studied in order to obtain new insights on mechanistic aspects concerning polyenic reaction. In this work, ultrafast pump−probe, transient anisotropy and continuous irradiation experiments of $CHTCl_8$ as well as DFT calculations are presented and compared to CHT as well as to other reactions with charged migrating particles.

2. Experimental Methods

$CHTCl_8$ has been prepared in-house according to a method described in ref 45 and its purity (≥95%) has been checked by ^{13}C NMR in $CDCl_8$ (Bruker, 250 MHz), IR spectroscopy with KBr pellets between CsI windows (Bruker IFS 113), and UV−vis spectroscopy (Varian, Cary 5e) and by the determination of its melting point (85 °C compared to 86 °C in ref 45). Since no IR data have been published for $CHTCl_8$, an FTIR spectrum is shown in Figure 1 while the frequencies were compared with DFT-calculations (B3-LYP/TZVP) using the program TURBOMOLE.[46−48] A comparison between calculated and experimentally determined vibrational frequencies is given in Table 1.

Femtosecond pump−probe and anisotropy experiments were carried out with a setup described previously.[28] In brief:

TABLE 1: Experimental and Theoretical IR Data of $CHTCl_8$[a]

	ν/cm^{-1} (theory)[b]	ν/cm^{-1} (expt)[c]		ν/cm^{-1} (theory)[b]
ν_1	1587.4	1552	ν_{21}	389.6
ν_2	1578.7	1542	ν_{22}	357.8
ν_3	1527.7	1500	ν_{23}	336.6
ν_4	1235.8	1229	ν_{24}	304.5
ν_5	1140.5	1147	ν_{25}	281.9
ν_6	1091.9	1107	ν_{26}	272.1
ν_7	1031.2	1057	ν_{27}	251.6
ν_8	976.5	969	ν_{28}	247.1
ν_9	960.6	969	ν_{29}	239.9
ν_{10}	803.7	819	ν_{30}	226.9
ν_{11}	760.7	790	ν_{31}	208.9
ν_{12}	727.8	745	ν_{32}	206.5
ν_{13}	671.4	677	ν_{33}	200.1
ν_{14}	663.5	664	ν_{34}	125.3
ν_{15}	654.5	647	ν_{35}	101.6
ν_{16}	636.1	624	ν_{36}	73.9
ν_{17}	626.2	612	ν_{37}	64.1
ν_{18}	520.6	508	ν_{38}	58.5
ν_{19}	467.8	469	ν_{39}	48.2
ν_{20}	394.2	n.a.		

[a] Both theoretical and experimental values are given for the first 19 values. The remaining frequencies (20−39) are experimentally not very well resolved, and therefore, only the theoretical values are given. [b] DFT calculations (B3-LYP/TZVP). [c] Experimental data in KBr.

femtosecond pulses were obtained from a commercial multipass amplifier system (FEMTOLASERS) that produced 30 fs pulses at a center wavelength of 795 nm and 1 kHz repetition rate.[49,50] The second harmonic was generated in a 100 μm BBO crystal (type I) and separated by dielectric mirrors from the fundamental. By collinearly recombining the fundamental and second harmonic beams, the third harmonic was generated in another 100 μm BBO crystal (type I). Because of uncompensated chirp, the time resolution was 60 ± 10 fs. The polarization of the probe beam was set either at 45° or at magic angle (≈54,7°) with respect to the pump beam by means of a $\lambda/2$ plate (Karl-Lamprecht). Intensities of the probe pulse before and behind the sample cell were detected by Si photodiodes (Hamamatsu) and the change of the optical density with and without pump pulse, ΔOD, was recorded. In anisotropy measurements, a Glan-Taylor polarizer (Alphalas) was used to simultaneously monitor the change of the optical density for the parallel, $\Delta OD_{\parallel}$, and perpendicular, $\Delta OD_{\perp}$, components. All experiments were performed in a flow-cell system at room temperature. The optical density was >4 to ensure that the pump beam was largely (1/e decay) absorbed within a thickness of <0.1 mm to avoid a noticeable group velocity mismatch between pump and probe pulses within the sample.[24] The concentration of CHT under these conditions was 10 mol/L in various solvents. In order to identify solvent effects, ΔOD values of the transient response were recorded in pure solvents in a 1 mm cuvette. In this case, the pump beam was not absorbed within 0.1 mm in contrast to dissolving $CHTCl_8$. By comparing these transients with those for CHT, we found a solvent contribution of about 5% in cyclohexane and *n*-hexane while it was almost 20% in 2,2,2-trichloroethanol (TCE).

Chemical reactions of $CHTCl_8$ under continuous irradiation were investigated by using a Hg/Xe arc lamp (Müller) that has two prominent lines at 263 and 275 nm; i.e., they are located within the absorption band of $CHTCl_8$. A home-built shutter system ensured the reproducibility of irradiation times such that the time intervals were identical for each experiment. $CHTCl_8$ solutions were filled into a 1 mm quartz cell and spectra were recorded by a UV−vis spectrometer (Varian, Cary 5e). Care

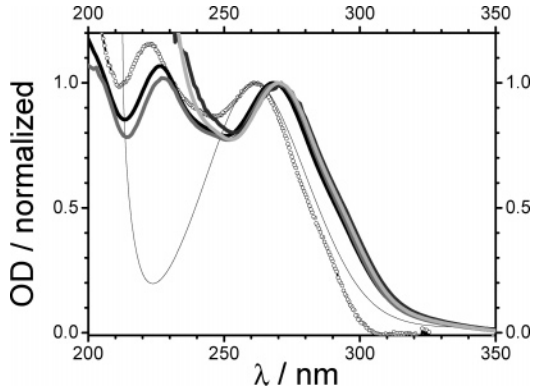

Figure 2. UV spectra of $CHTCl_8$ in isopropanol (black curve), trichloroethanol (dark gray), cyclohexane (gray), and chloroform (light gray). The open circles show its gas-phase spectrum under saturated vapor pressure at ~100 °C. The thin line is a spectrum of CHT in cyclohexane.

was taken to maintain a constant photon flux in the sample by controlling the lamp current.

3. Results and Discussion

3.1. Steady-State Measurements. Figure 2 represents the gas-phase steady-state UV−vis spectrum of $CHTCl_8$ at saturated vapor pressure at ~100 °C in (open circles). It shows two absorption maxima at $\lambda_1 = 262$ nm and $\lambda_2 = 222$ nm, which can be considered to be $\pi^* \leftarrow \pi$ transitions in analogy to CHT.[51] In solution, these maxima are red-shifted to $\lambda_1 = 270$ nm (271 nm in TCE and 268 nm in isopropanol) and $\lambda_2 = 227$ nm. The corresponding spectra are shown in Figure 2 as thick solid lines. In chloroform and TCE, λ_2 is masked by absorption bands of the solvents. On the other hand, one finds for CHT $\lambda_1 = 255$ nm (261 nm) and $\lambda_2 = 194$ nm (199 nm) in the gas phase (values for cyclohexane as solvent are given in brackets).[52] The spectrum exhibits a band shape similar to $CHTCl_8$ but blue-shifted (see thin black line in Figure 2) since chlorine atoms are lowering the energy of the conjugated π-system.[53] The absorption coefficient at λ_1 was determined to $\epsilon_1^{CHTCl_8} = 5100$ L mol^{-1} cm^{-1} for $CHTCl_8$[54] ($\epsilon_1^{CHT} = 3100$ L mol^{-1} cm^{-1}),[52] while λ_2 is much smaller for the perchlorinated species ($\epsilon_2^{CHTCl_8} = 6500$ L mol^{-1} cm^{-1} [54] compared to $\epsilon_2^{CHT} = 17\,800$ L mol^{-1} cm^{-1}).[55]

3.2. Pump—Probe Measurements. Pump−probe and transient anisotropy experiments in different solvents were performed using 263 nm pump and 395 nm probe pulses. Figure 3 shows pump−probe measurements under magic angle conditions in TCE (upper triangles) and cyclohexane (lower triangles). Time constants were extracted using the following model adopted from the CHT dynamics:[24]

$$CHTCl_8 \xrightarrow{\tau_0} CHTCl_8^{(1A'')} \quad (1)$$

$$CHTCl_8^{(1A'')} \xrightarrow{\tau_1} CHTCl_8^{(2A')} \quad (2)$$

$$CHTCl_8^{(2A')} \xrightarrow{\tau_2} CHTCl_8^* \quad (3)$$

$$CHTCl_8^* \xrightarrow{\tau_3} CHTCl_8 \quad (4)$$

$CHTCl_8^{(1A'')}$ and $CHTCl_8^{(2A')}$ denote molecules in the 1A″ and the 2A′ states, respectively, $CHTCl_8$* represents the vibrational hot ground state, τ_0 is characterized by the temporal resolution and the τ_i are the time constants for the various relaxation processes. Note that this model leads to a three-exponential decay, while the one used for CHT[24] did not distinguish between τ_1 and τ_2 because τ_1, i.e., the time constant for the 1A″−2A′ transition, was supposed to be faster than the time resolution of the experiment. Therefore, we will denote the 1A′−1A″ transitions in CHT by τ_{IC}^{CHT} combining τ_1 and τ_2.

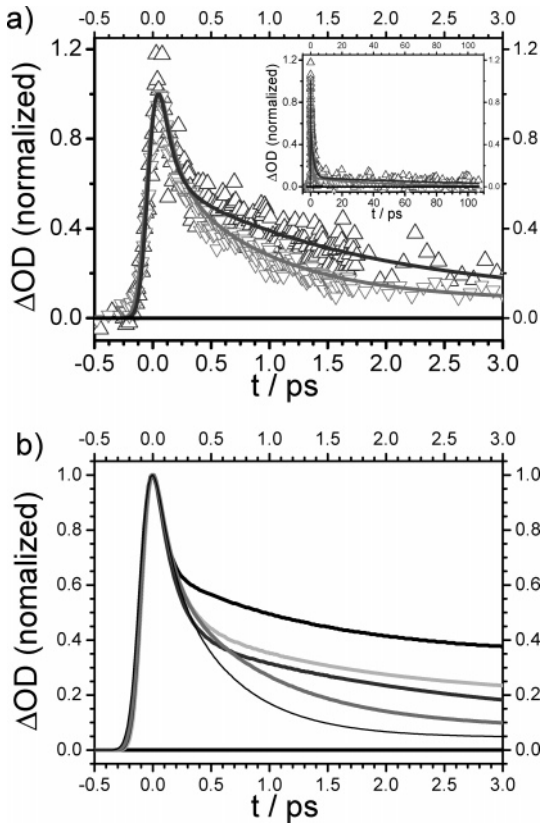

Figure 3. (a) Comparison of magic angle measurements of $CHTCl_8$ in trichloroethanol (dark gray) and cyclohexane (gray). The pump wavelength was 263 nm and the probe wavelength 395 nm. (b) Magic angle measurements of $CHTCl_8$ in various solvents (isopropanol (black curve), *n*-hexane (thin black), trichloroethanol (dark gray), cyclohexane (gray), chloroform (light gray)) at the same wavelengths. For clarity, only the normalized fits are shown.

Measurements of $CHTCl_8$ have been performed in five different solvents (*n*-hexane, cyclohexane, TCE, chloroform, and isopropanol) and the resulting time constants are given in Table 2. While at early times ($t < 150$ fs) the transient response is comparable for all solvents, the profiles are clearly different on a longer time scale. A more quantitative analysis using eqs 1−4 reveals that for unpolar solvents (i.e., *n*-hexane and cyclohexane), τ_2 is a factor of 1.5 shorter than for the polar solvents chloroform and isopropanol and a factor of 2 shorter compared to TCE. The third time constant, τ_3, attributable to vibrational relaxation, i.e., equilibration with the surrounding medium was >60 ps for all solvents. Since a more detailed analysis of vibrational relaxation requires wavelength dependent measurements, it will be omitted in the following discussion.[56]

From the analysis of the transients in terms of eqs 1-4 and in analogy to the CHT system we tentatively assign the [1,7]-sigmatropic Cl-migration in $CHTCl_8$ to occur at the second conical intersection. This is further substantiated by our recent pump−probe experiments on CHT and its perdeuterated counterpart $CHTd_8$ where a time constant of $\tau_{IC}^{CHT} = 110 \pm 10$ fs and $\tau_{IC}^{CHTd_8} = 150 \pm 15$ fs was attributed to the corresponding H (D) migration.[28] The difference between these two constants was explained by a simple energetic picture implying $\tau_{IC} \propto \sqrt{\mu}$, where μ is the reduced mass which can be approximated

TABLE 2: Time Constants for $CHTCl_8$ after Excitation at 263 nm and Probing at 395 nm in Different Solvents[a]

solvent	τ_1/fs[b]	τ_2/fs[b]	τ_3/ps	τ_1^b/fs	τ_2^b/ps	r_0	μ/D	$F(\epsilon_0,n)$
n-hexane	135 ± 20	905 ± 150	>60	150	6	0.27	0	0
cyclohexane	145 ± 20	900 ± 150	>60	120	7	0.30	0	0
TCE	130 ± 20	1845 ± 200	>60	135	8	0.30	>3[c]	0.51
chloroform	140 ± 20	1420 ± 200	>60	120	10	0.25	1.16	0.29
isopropanol	130 ± 20	1460 ± 200	>60	100	5	0.30	1.85	0.63

[a] The τ_is are the time constants for the pump-probe spectroscopy, The τ_i^as are the time constants for the anisotropy decay and r is the time zero anisotropy. Also listed are the dipole moment μ of the solvents and the dielectric measure of the solvent $F(\epsilon_0,n)$, calculated by eq 7. [b] The errors for the τ_is are estimated by the deviations of several measurements, which exceed the χ^2-deviation of a Levenberg−Marquardt algorithm by a factor of 2. [c] 2,2,2-Trichoroethanol has two isomeric forms (cis and trans) with different dipole moments. For a brief discussion of the given value, see Appendix A.2 and ref 80.

TABLE 3: Ab Initio Calculations of the Moments of Inertia I_i, Correlation Times for Free Rotational Motion ($\tau_{c,i} = (2\pi/9)(I_i/k_BT)^{1/2}$ (see Ref 83) at Room Temperature, and the Zero-Point Corrected Energy Barriers.

	CHT	$CHTCl_8$
moments of inertia/kg m^2	$I_A = 2.273 \times 10^{-45}$	$I_A = 3.093 \times 10^{-44}$
	$I_B = 2.275 \times 10^{-45}$	$I_B = 2.769 \times 10^{-44}$
	$I_C = 4.157 \times 10^{-45}$	$I_C = 4.381 \times 10^{-44}$
correlation time/ps	$\tau_{c,A} = 0.52$	$\tau_{c,A} = 1.91$
	$\tau_{c,B} = 0.52$	$\tau_{c,B} = 1.80$
	$\tau_{c,C} = 0.70$	$\tau_{c,C} = 2.27$
energy barrier ΔE_{gs-ts}		
[1,7]-shift	267 kJ/mol	117 kJ/mol
[1,5]-shift	155 kJ/mol	78 kJ/mol

by the mass m of the migrating particle (i = H, D, or Cl). From this, one would expect a combined time constant of $\tau_{IC}^{CHTCl_8} = 110\ \text{fs}\cdot\sqrt{m_{Cl}/m_H} \approx 650$ fs for $CHTCl_8$. Inspection of the first two time constants of $CHTCl_8$ in nonpolar solvents (cyclohexane and *n*-hexane) gives $\tau_1 = 140$ fs and $\tau_2 = 900$ fs, respectively. This can be combined to one time constant $\tau_{IC}^{CHTCl_8}$ of ∼ 720 fs which is only 10% higher than the expected time constant of our oversimplified model.[57]

An analysis of the transients in various solvents reveals a more complex situation. According to the time constants given in Table 2, τ_2 roughly increases with increasing polarity of the solvent (for a more detailed analysis, see part 3.5). If we identify the time constant to be attributable to the [1,7]-Cl migration, polar solvents lead to a retardation of the chlorine shift. This in turn indicates a charge separation within the $CHTCl_8$ molecule that is stabilized by polar solvents. These findings are supported by theoretical treatments (see part 3.3).

3.3. DFT Calculations. Comparing the pump−probe data for CHT and $CHTCl_8$, one of the main differences is the behavior in various solvents: While no solvent dependence of the time constants has been reported for CHT,[24] this is not the case for the perchlorinated species. For a better understanding, DFT calculations (B3-LYP/TZVP if not mentioned otherwise) of the ground and transition states of the photochemically allowed suprafacial [1,7]-Cl (-H) and the thermally allowed suprafacial [1,5]-Cl (-H) migrations[44] have been performed. The results are given in Tables 3 and 4. Illustrations of the ground state and the two transition states are given in Figures 4 and 5. In the ground state, both molecules belong to the C_s symmetry group. The angles between the plane defined by the atoms C1, C2, C5, and C6 and the C_2H_2 (C_2Cl_2) group (α_1) or the CH_2 (CCl_2) group (α_2), respectively, are $\alpha_1 = 31°$ and $\alpha_2 = 66°$ for CHT and become slightly larger ($\alpha_1 = 38°$ and $\alpha_2 = 67°$) in $CHTCl_8$. A Mullikan population analysis of the ground state shows no unusual charge distribution for both molecules while for the [1,7]- as well as for the [1,5]-transition states, the migrating chlorine atom carries a considerable amount of charge (−0.32 for BP/SV(P), −0.42 for B3-LYP/TZVP for the [1,7]- and −0.30 for the [1,5]-migration; see Table 4). These results

TABLE 4: Mulliken Charges for the Ground State (g.s.) and the [1,7]- and [1,5]-Transition States for CHT and $CHTCl_8$[a]

	CHT g.s.[b]	CHT [1,7][c]	CHT [1,7][b]	CHT [1,5][c]
C1	−0.1351	−0.0794	−0.0429	−0.0982
C2	−0.0897	−0.1190	−0.1962	−0.1129
C3	−0.1477	−0.0369	−0.0770	−0.0969
C4	−0.1435	−0.1301	−0.1767	−0.2232
C5	−0.0932	−0.0377	−0.0802	−0.0484
C6	−0.1309	−0.1205	−0.1974	−0.1052
C7	−0.2614	−0.0802	−0.0484	−0.2195
H8	0.1256	0.1196	0.1655	0.1223
H9	0.1211	0.0645	0.1019	0.1158
H10	0.1154	0.0810	0.1123	0.1214
H11	0.1149	0.0593	0.1021	0.1527
H12	0.1207	0.0807	0.1125	0.1196
H13	0.1260	0.0646	0.1020	0.1182
H14	0.1127	0.1200	0.1672	0.1525
H15	0.1650	0.0142	−0.0447	0.0538
	$CHTCl_8$ g.s.[a]	$CHTCl_8$ [1,7][b]	$CHTCl_8$ [1,7][a]	$CHTCl_8$ [1,5][a]
C1	−0.0916	0.0205	−0.0395	0.0130
C2	−0.0106	0.0325	0.0454	0.0538
C3	−0.0266	0.0374	0.0312	0.0174
C4	−0.0283	−0.0034	−0.0943	−0.1090
C5	−0.0108	0.0354	0.0311	0.0395
C6	−0.0899	0.0352	0.0446	0.0392
C7	0.0792	0.0222	−0.0370	−0.1072
Cl8	0.0445	0.0365	0.0800	0.0497
Cl9	0.0140	0.0178	0.0665	0.0405
Cl10	0.0182	0.0148	0.0499	0.0494
Cl11	0.0186	0.0061	0.0473	0.0717
Cl12	0.0143	0.0154	0.0498	0.0329
Cl13	0.0448	0.0174	0.0664	0.0497
Cl14	0.0208	0.0366	0.0800	0.0716
Cl15	0.0034	−0.3245	−0.4214	−0.3004

[a] The numeration is defined in Figures 4 and 5. The migrating atoms are H15 and Cl15, respectively. [b] (B3-LYP/TZVP). [c] (BP/SV(P)).

support our assumption that in the case of $CHTCl_8$ a charge separation occurs during the atom shift. Moreover, the activation energies for the [1,7]- and the [1,5]-migration of $CHTCl_8$ are significantly lower than for CHT (by 112 and 39 kJ/mol, respectively). Please note that in these calculations neither nonadiabatic processes between different potential energy surfaces nor entropic influences were incorporated, and hence, accurate single point calculations for the transition states that are supposed to be located in a conical intersection (or weakly avoided crossing) are difficult to determine.[18] This might explain the discrepancy between the experimental value for the [1,7]-H shift (458 kJ/mol)[52] and the theoretical value using DFT-calculations (267 kJ/mol). Interestingly, the experimental value also differs signifcantly from ab initio calculations performed by Steuhl et al.[26] (443 kJ/mol for CASSCF/3-21G, 399 kJ/mol for CASSCF/6-31G*, 337 kJ/mol for MNDOC-CI, 314 kJ/mol for CASPT2/ANO) where nonadiabatic influences are explicitly incorporated. Therefore, these results show the current limitation of theoretical techniques. For example, the method which gives

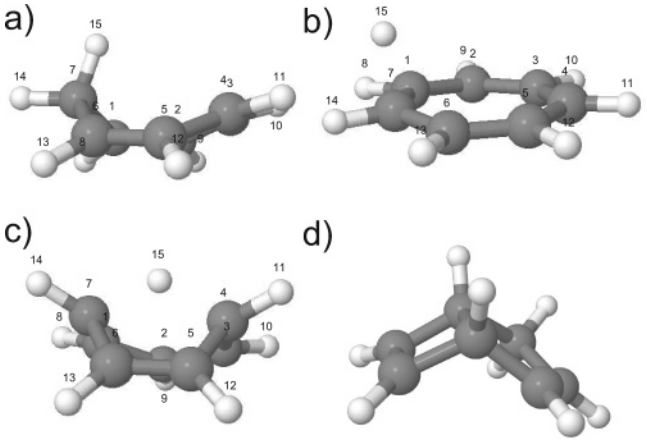

Figure 4. Geometries for the (a) ground state, (b) [1,7]-transition state and (c) [1,5]-transition state geometry of CHT using DFT (B3-LYP/TZVP) calculations. (d) Ground state geometry of BHD.

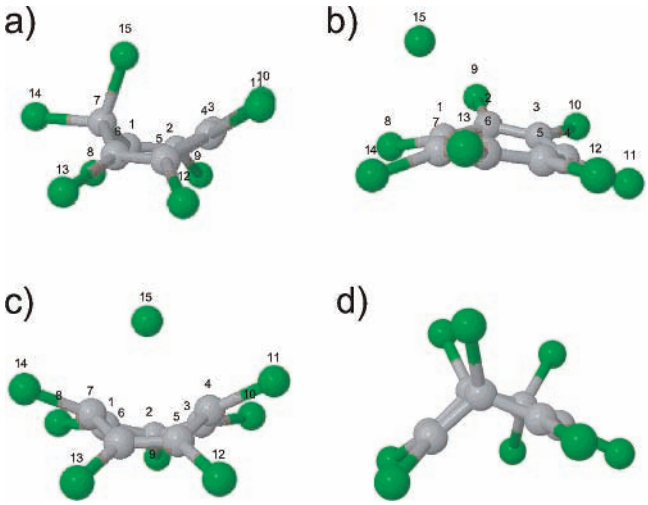

Figure 5. Geometries for the (a) ground state, (b) [1,7]-transition state, and (c) [1,5]-transition state geometry of $CHTCl_8$ using DFT (B3-LYP/TZVP) calculations. (d) Ground state geometry of $BHDCl_8$.

the best agreement with the experimental excitation energy (CASSCF/3-21G) gives the largest deviation from the barrier in the 2A′-state, which is probably incorrect.[26,27] In all cases, the value for theoretically calculated [1,7]-energies are too small. In particular, DFT calculations relying on the adiabatic approximation as presented in this work give (not surprisingly) the largest deviations with 41% of the experimental value.

Certainly, absolute values for the barriers obtained by DFT calculations have to be taken with care; nevertheless, the general trend by continuous substitution of H by Cl atoms may be instructive. Therefore, ground and transition state geometries and energies for a set of different chlorinated CHT derivatives were calculated. The number of chlorine atoms was increased starting at the saturated C atom (i.e., 7-CHTCl, 1,7,7-$CHTCl_3$, 1,6,7,7-$CHTCl_4$ etc.). The results are given in Table 5. With decreasing number of Cl atoms, the molecule is less tilted while the difference in activation barriers $\Delta E_i = E_i^{[1,7]} - E_i^{[1,5]}$ between the [1,7]- and the [1,5]-transition states reduces and becomes negative for six chlorine atoms or less. Furthermore, the migrating chlorine atom is charged in all cases and a Mullikan population analysis reveals that the amount of charge is nearly identical (-0.32 ± 0.02 for the [1,7]-migration using BP/SV(P)). In agreement with our results, Okajima et al. earlier found that for 1,7,7-trichlorocycloheptatriene the activation energy for a [1,7]-chlorine shift is lower than the energy for a [1,5]-chlorine shift (49.2 vs 68.3 kJ/mol) also using DFT calculations (B3-LYP/6-311+G**).[43] They assumed a fast, thermally allowed [1,7]-chlorine migration to explain the behavior in NMR measurements. If the nonadiabatic correction are not significant, this reaction contradicts the Woodward−Hoffmann rules[44] where a sigmatropic [1,7]-shift is only photochemically allowed, but not thermally. For $CHTCl_7$ and $CHTCl_8$, however, no contradiction to the Woodward−Hoffmann rules is expected (see Table 5).

3.4. Anisotropy Measurements. Transient anisotropy measurements have been performed in the same solvents as the pump−probe experiments and the temporal evolution of the anisotropy has been calculated using the following equation[58]

$$r(t) = \frac{\Delta OD_{||}(t) - \Delta OD_{\perp}(t)}{\Delta OD_{||}(t) + 2\Delta OD_{\perp}(t)} \tag{5}$$

where $\Delta OD_{||}$ and $\Delta OD_{\perp}$ are described in the experimental section. Typical anisotropy profiles are shown in Figure 6. At a first glance, the process can be considered to be biexponential with time constants τ_1^a and τ_2^a. The corresponding time constants and the time zero anisotropies are given in Table 2. One realizes that the anisotropy behavior, especially τ_1^a, does hardly depend on the solvent; it is therefore possible to determine a solvent independent time constant $\tau_1^a = 120 \pm 20$ fs, which is close to τ_1 in the pump−probe studies. Moreover, the time zero anisotropy for all solvents is 0.28 ± 0.03 and 0.35 ± 0.03 after deconvolution (see Figure 6). As expected, the deconvolution increases the initial anisotropy.[59] Again, a comparison with the values for CHT[28] is instructive. First, the initial anisotropy for $CHTCl_8$ is remarkably smaller (~0.3 compared to ~0.6 for CHT). In CHT, the anomalous high anisotropy was explained by a quasi-degeneracy of excited states; i.e., the molecule is considered to be excited in the vicinity of a conical intersection. The absence of such coherence effects indicates that the 1A″−2A′ transition of $CHTCl_8$ is not in the Franck−Condon region leading to a substantially lower initial anisotropy. From this finding, one can also enlighten the time zero anisotropy in CHT. Considering the Perrin equation[60]

$$r(t=0) = \frac{1}{5}(3\langle\cos^2\beta\rangle - 1) \tag{6}$$

one can calculate the angle β defined by the orientation of the pump and the probe transition dipole moments ($\vec{\mu}_{pump}$ and $\vec{\mu}_{probe}$), i.e., in this case $\beta^{CHTCl_8} = 17°$. Because of analogue structures and the same symmetry of CHT and $CHTCl_8$, this angle is supposed to be similar. However, the effect of quasi-degeneration has to be considered. In ref 61, this is treated in more detail, so only the relevant aspects shall be summarized here. If the 1A″ and the 2A′ states were degenerate, CHT would be excited to a state $|e\rangle = a|1A''\rangle + b|2A'\rangle$ whose transition dipole moment possessed the greatest projection onto the *z*-axis, i.e., the polarization axis of the pump pulse (here $a^2 + b^2 = 1$). Such a model leads to a time zero anisotropy of $r(0) = 0.7$.[61] This is consistent with other models[62−64] and has also been demonstrated experimentally for the case of MgTPP.[65] If one of the excited states is dark, it cannot be reached by a one-photon process; however, it can couple nonadiabatically via a conical intersection (or weakly avoided crossing) with the bright state. This coupling can be described by a mixing angle between these two states. Furthermore, since CHT has no geometrical restrictions due to group theory (e.g., MgTPP has D_4-symmetry which determines the relative orientation of the transition dipole moments), $\vec{\mu}_{pump}$ and $\vec{\mu}_{probe=|e\rangle}$ may include any angle. Setting

TABLE 5: Activation Energies for the Chlorine Migration and Characteristic Angles of Several Substituted Chlorinated CHT Derivatives[a]

molecule	$E^{[1,7]}$/kJ·mol^{-1}	$E^{[1,5]}$/kJ·mol^{-1}	ΔE/kJ·mol^{-1}	α_1/deg	α_2/deg
7-CHTCl	42.8	97.1	−44.3	44.4	19.0
1,7,7-CHTCl$_3$	50.2	76.8	−26.6	47.4	19.9
1,6,7,7-CHTCl$_4$	53.5	72.0	−18.5	59.3	24.4
1,2,6,7,7-CHTCl$_5$	57.3	68.1	−8.8	61.4	25.9
1,2,5,6,7,7-CHTCl$_6$	65.4	67.4	−2	63.5	27.6
1,2,3,5,6,7,7-CHTCl$_7$	75.0	65.9	9.1	64.8	30.7
CHTCl$_8$	95.8	69.5	26.3	67.0	38.0

[a] α_1 and α_2 denote the torsion angles of the C7 and C3−C4 atoms out of the C1−C2−C5−C6 plane (compare the numbering system with Figure 5). The calculations were performed with DFT (BP/SV(P)). 7,7-CHTCl$_8$ is missing due to convergence problems of the transition states.

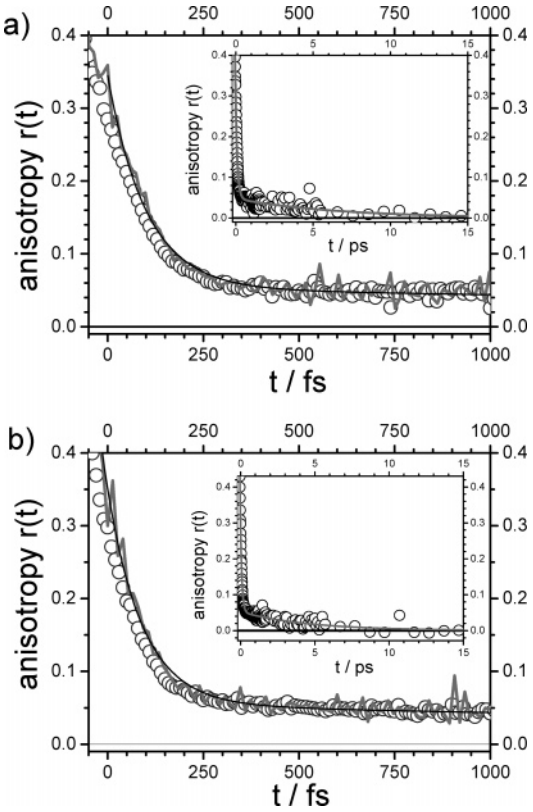

Figure 6. (a) Transient anisotropy of CHTCl$_8$ in cyclohexane. The circles are the originally recorded traces, while the gray curve is the deconvolution of the response and the black curve is a biexponential fit of the deconvolution. The deconvolution procedure was carried out by the method described in ref 84. In the inset, the response is shown on a longer time scale. Here, the gray curve is a biexponential fit. The pump wavelength was 263 nm, the probe wavelength 395 nm. (b) Same as in part a, but in isopropanol as solvent.

this angle $\beta^{\mathrm{CHTCl_8}} = 17°$, a minimum value of the mixing angle of 12° is obtained, which is close to the results for parallel dipole moments.[61] Note that this angle depends on the orientation of all three transition dipole moments, so only a lower limit can be given here.

It should be noted that the first time constant τ_1^a for CHTCl$_8$ is comparable to τ_1 derived from the transient anisotropy of CHT (and CHTd$_8$), where a time constant of 150 fs (180 fs) has been found,[28] but considerably faster than the free rotational reorientation time of CHTCl$_8$ (see Table 3) and the Cl-migration process. Additionally, the anisotropy does not exhibit the typical Gaussian behavior at early times supporting the fact that molecular rotation is not the reason for this fast decay. Hippler et al. suggested the anisotropy decay to be limited by the pseudorotation of the hydrogen (deuterium) atom.[28] This limit is still valid in the case of CHTCl$_8$, but the anisotropy decays much faster than the corresponding chlorine shift. A possible interpretation is as follows: After excitation, the molecule is expected to vibrate strongly in the 1A″ state before reaching the transition state of the [1,7]-migration (1A′−2A′ transition). Therefore, vibrational motions in the excited states are necessary to "prepare" the molecule for the [1,7]-shift, which leads to a fast decrease of the anisotropy within 120 fs while the Cl-shift is slower.

The second time constant τ_2^a is attributed to rotational diffusion and chlorine migration. Rotational diffusion mainly depends on the friction of the molecule in the solvent whereas the chlorine shift leads to a pseudorotation of the molecule which causes an additional displacement of the transition dipole moment and hence an anisotropy decay. These two processes are not separable with transient anisotropy measurements. However, since τ_2^a is longer than τ_2 in the pump−probe experiments and shows no clear solvent dependency, it will be primarily assigned to reorientation dynamics.

3.5. Discussion of the Femtosecond Dynamics. The most obvious feature of the femtosecond dynamics of CHTCl$_8$ is the solvent dependence of τ_2 in the pump−probe studies, which might be due to an ultrafast charge transfer during the [1,7]-shift. If this is the case, one ansatz is that the migrating chlorine atom carries a considerable amount of negative charge, which is also supported by ab initio calculations. Note that the calculations of CHT show no charge of the migrating H atom which correlates with the fact that its dynamics exhibit no solvent dependence.[28] To explain the different time constants for τ_2 under the assumption of a charged chlorine atom, various influences have to be considered.

One important aspect is the dipole moment of various solvent molecules as given in Table 2, since it couples directly to the charged atom. In nonpolar solvents such as cyclohexane or *n*-hexane, the reaction is fastest, while in polar solvents, the reaction is significantly slowed down. One would therefore expect that a higher dipole moment leads to a slower reaction. This is true for TCE, which shows the greatest effective dipole moment (see section A.2 for a discussion on the structure and dipole moment of pure TCE) and the largest time constant τ_2. However, the magnitude of the dipole moment is not the only determining factor since the dynamics of CHT in chloroform and isopropanol occur on a comparable time scale while their dipole moments are clearly different (see Table 2). The reason for this behavior might be the activation entropy of the barrier in the S_1-state which is supposed to be smaller for chloroform than for isopropanol/TCE since chloroform is the smallest molecules in this series. From this one might argue that the solvation shell contains a larger number of molecules that influences the transition state geometry and the spectral response function; the latter is a measure of the solvent reorientation time after excitation of a solute and is known to be much faster for chloroform[66] leading to a deceleration of the reaction rate compared to isopropanol. Thus, the entropy effect may com-

pensate the lower dipole moment leading to equal time constants, τ_2, for the chlorine shift in $CHTCl_8$ in chloroform and isopropanol.

From these findings, one can conclude that the mechanism for the [1,7]-Cl migration is governed by an intramolecular charge transfer in the excited state. Therefore, it seems instructive to compare this reaction mechanism with an intramolecular proton transfer in the excited state (ESIPT), which represents an important class of reaction involving charged migrating particles. One of the fundamentals to explain ESIPT-dynamics is Marcus' theory.[67,68] The proton transfer occurs between the first excited states of the normal and the tautomeric form of a molecule.[69,70] The barrier height between these two states is determined by the solvent induced barrier ($\Delta G^{\ddagger}$). This height is given by $\Delta G^{\ddagger} = (\lambda/4)(1 + \Delta G/\lambda)^2$ where

$$\lambda = \frac{(\vec{\mu}_N - \vec{\mu}_T)^2}{r^3} F(\epsilon_0, n) \qquad (7)$$

is the reorganization energy of the solvent which can be obtained by the Onsager cavity model.[71] Here, $\vec{\mu}_i$ are the dipole moments of the normal (N) and the tautomeric (T) form, r is the radius of the molecule (which is supposed to be spherical) and $F(\epsilon_0,n)$ is the static response function of the solvent. The values for the different solvents are given in Table 2. Using this ansatz, one would expect the dynamics of $CHTCl_8$ to be slowest in isopropanol (which is not the case). The main difference between ESIPT and the $CHTCl_8$ mechanism is that in $CHTCl_8$, the "tautomeric" form is not in the excited state, since the migration takes place at the $1A'-2A'$ intersection, i.e., between the excited and ground state and not exclusively in the excited state. Moreover, the barrier in the first excited state ($2A'$) of $CHTCl_8$ is not of Marcus' type. Altogether, the [1,7]-Cl migration is a process where the photochemically induced shift of a charged atom cannot be described by the ESIPT-mechanism.

In recent years, several sigmatropic hydrogen migrations have been studied, but besides the [1,7]-H-migration of CHT, all of them were [1,3]-shifts[9,72,73] either on dienes such as cyclopentadiene[9] or systems with a single double-bound such as cyclohexene[72] or bicyclo[2,1,1]heptene.[73] The [1,3]-shift in cyclopentadiene is similar to the [1,7]-shift observed in CHT because in both cases two conical intersections and a competing electrocyclization are involved (see section 3.6).[9] Perhalogenation of this species should give similar results as presented in this paper. The same is true for cyclohexene while the hydrogen migration in bicyclo[2,1,1]heptene is always followed by a C-migation and therefore another product. Migration of charged groups have been studied in a photo-Fries rearrangement.[74] However, the reaction proceeds much slower (≈13 ps) than the [1,7]-H shift of CHT, and no solvent dependent measurements have been performed.

In conclusion, this work reveals the first ultrafast study of a chlorine migration.[75] It predicts the migration to depend on the dipole moment of the solvent and entropic influences (which depend on the reorientation times). The mechanism is clearly different from proton-transfer reactions. The analysis allows for a localization of the migrating step. Since the first time constant ($\tau_1^{CHTCl_8} = 140$ fs) in the pump−probe studies is solvent independent, there is neither a charge separation nor can the solvent interact with the charged complex on this time scale. Also, the anisotropy significantly decays on a comparable time scale indicating the importance of vibrational motions in the excited-state before the transition state for the [1,7]-Cl migration is reached. The chlorine shift then takes place at the $1A'-2A'$ intersection, i.e., at the second conical intersection in agreement with the mechanism proposed for CHT.[22,26,27] However, in the case of $CHTCl_8$ it shows a pronounced solvent dependence. Unfortunately, the chlorine migration is not clearly resolvable by anisotropy experiments, since vibrational motions upon excitation result in an anisotropy decay which is faster than the migration process, leaving only small positive anisotropy values after delay times exceeding 0.3 ps. Therefore, the decay of this residuary anisotropy (τ_2^a) may be explained by a superposition of the chlorine shift and by reorientation of $CHTCl_8$ as the rotational correlation times (see Table 3) are on the same time scale as the migration.

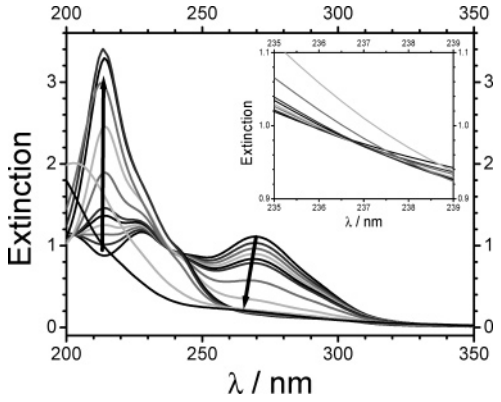

Figure 7. UV-absorption spectra of $CHTCl_8$ in cyclohexane. The different spectra were taken after irradiation with a Hg/Xe arc lamp. The irradiation times were 0, 1, 2, 3, 4, 5, 10, 20, 50, 100, 200, 500, and 1000 s. Arrows indicate the shift with increasing time. The inset highlights the isosbestic point around 237 nm.

3.6. Continuous Irradiation Experiments. In order to study competition reactions of $CHTCl_8$ after photoexcitation and to obtain a more profound understanding of the potential energy surface involving photochemically allowed transitions, continuous irradiation measurements were performed in various solvents. After certain time intervals, spectra between 200 and 350 nm were recorded. In Figure 7, a typical irradiation measurement of $CHTCl_8$ in cyclohexane is shown. Initially, the steady-state spectrum is obtained (see Figure 2) while at longer irradiation times the spectral evolution of the system is observed. With the decrease of the characteristic peak at 270 nm a new absorption band, peaking at 214 nm, arises. Moreover, an isosbestic point can be seen at 237 nm for irradiation times $t < 20$ s (see inset of Figure 7). The same irradiation measurements have been performed in isopropanol, TCE, and chloroform. In Figure 8, the temporal evolution at the absorption maximum of $CHTCl_8$ at 270 nm (268 nm for isopropanol and 271 nm for TCE) is shown. Note that the time constants of these measurements (solid lines are biexponential fits to guide the eye) have no physical meaning, since the photon flux is not exactly known. Therefore, the branching ratio between the [1,7]-migration and the [4,5]-electrocyclization cannot be determined absolutely from these experiments. Relatively, the decay in cyclohexane is three times faster than in chloroform or isopropanol and eight times faster than in TCE. At longer times, the optical density (OD) increases for all solvents which is most pronounced for TCE. For comparison, a measurement of CHT in cyclohexane at the absorption maximum at 261 nm has been added to Figure 8. The dynamics are a factor 100 slower than for $CHTCl_8$. When considering the $CHTCl_8$ spectra (measured at $\lambda > 200$ nm for isopropanol and cyclohexane, $\lambda > 230$ nm for chloroform and $\lambda > 235$ nm for TCE) one finds isosbestic points for cyclohexane and chloroform at 237 nm while in isopropanol, this point is blueshifted by 9 nm at 228 nm and not as pronounced

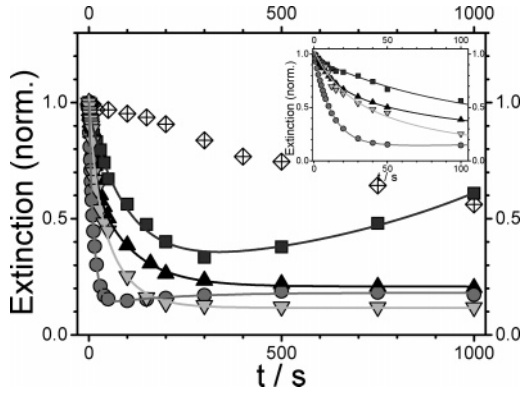

Figure 8. Normalized optical density (OD) of $CHTCl_8$ in cyclohexane (circles), chloroform (lower triangles), isopropanol (upper triangles) and 2,2,2-trichlorethanol (squares) at the absorption maximum of $CHTCl_8$ at 270 nm (268 nm for isopropanol) after irradiation with a Hg/Xe arc lamp. A biexponential fit is added to guide the eye. The rhombs are measurements of CHT in cyclohexane at the absorption maximum at 261 nm.

as in the former solvents. In TCE, the isosbestic point is red-shifted by 2 nm to 239 nm and is, as in isopropanol, not very sharp.

The isosbestic point indicates the formation of a new chemical species. To characterize this product, ^{13}C NMR spectra in $CDCl_3$ were recorded. The main peaks could be assigned to $CHTCl_8$ (δ = 84.3, 129.2, 134.1, 134.5 ppm) and octachloro bicyclo-[3.2.0]-hepta-2,6-diene ($BHDCl_8$, δ = 78.7, 81.8, 89.0, 132.2, 133.5, 134.2, 137.5 ppm, see ref 76 for comparison). Additional peaks (around 20) between $\delta = 137-129$ ppm and $\delta = 78-89$ ppm were also observed, but with at least 10 times weaker intensities compared to the main bands. These weak peaks were assigned to polymer structures, since the formation of white needles could be detected after sufficient long irradiation time (several hours). Two further small peaks at δ = 94.8 ppm and δ = 95.0 ppm indicate the presence of perchlorotoluene. Additionally to the NMR experiments, the absorption spectra after 50 or 100 s can be compared to the spectrum of $BHDCl_8$ in ref 77, which shows a maximum at the same wavelength as the species formed in the continuous irradiation experiments (214 nm; extinction coefficient $\epsilon = 10^4$ L mol^{-1} cm^{-1}). This suggests the competition reaction to be intramolecular, e.g., a photochemically allowed [4,5]-electrocyclization, which can also be found in CHT.[31] When heating the samples at 333 K, no change of the optical absorption spectrum could be detected in cyclohexane within 2 days, while in polar solvents, $BHDCl_8$ is formed quantitatively.

DFT calculations of the ground state energies of the possible photoproducts of CHT and $CHTCl_8$ are summarized in Figure 9 and a sketch of the geometry-optimized ground state structures of BHD and $BHDCl_8$ is shown in Figures 4 and 5, respectively. One recognizes that the energetic differences between various chlorinated species are smaller than for the perhydrogenated variant. Moreover, it turns out that the perchlorinated bicyclo product, $BHDCl_8$, is energetically more stable than $CHTCl_8$, in contrast to the CHT system. This explains the product-forming process upon heating of $CHTCl_8$ in polar solvents. Obviously, there exists a nonradiative reaction mechanism which is promoted by the polarity of the solvent leading to the thermodynamically more stable product (i.e., $BHDCl_8$). In the solvent cyclohexane, such a reaction path does not exist since $CHTCl_8$ does not react.

The results from femtosecond experiments, continuous irradiation experiments of $CHTCl_8$ in different solvents, and ab initio calculations can be summarized as a sketch of the potential

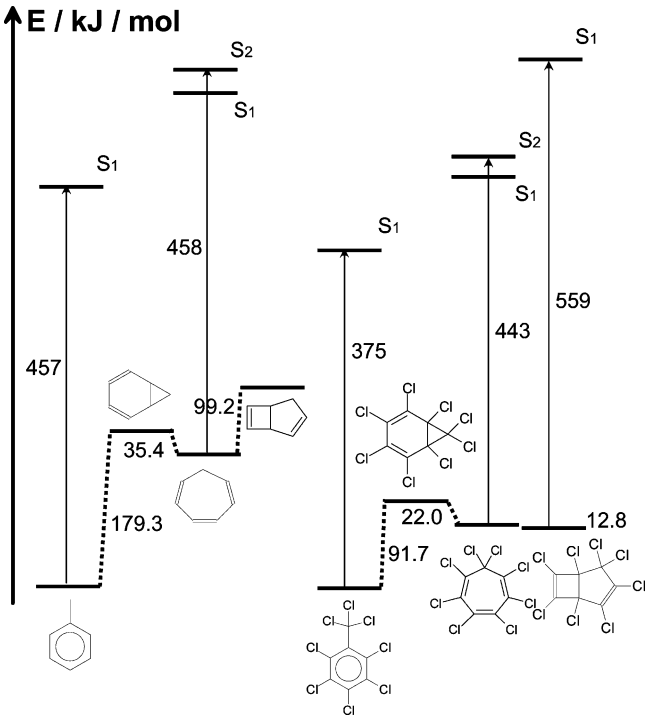

Figure 9. Potential energy diagram of CHT and $CHTCl_8$ and photoproducts as received by DFT (B3LYP/TZVP) calculations. The excited states are added using the experimental excitation energies.[55,77]

energy surface (Figure 10). After photoexcitation, the molecule reaches the 2A′ state via a conical intersection, where a competition reaction between the [1,7]-chlorine shift and the formation of $BHDCl_8$ takes place. Note that the formation of $BHDCl_8$ may also proceed from the energetically hot ground state, but this seems unlikely for the following reason: After irradiation of $CHTCl_8$, the formation process of $BHDCl_8$ is fastest in the nonpolar solvent cyclohexane. If the reaction would take place in the vibrationally hot ground state, one would expect this reaction to be the fastest when heating the sample. Clearly, this is not case, since the reaction does not occur at 333 K. The reaction in polar solvents at higher temperatures may proceed via an alternative mechanism as competition to a thermally allowed [1,5]-migration. This migration should be favored in polar solvents as the migrating chlorine atom is charged (see Table 4). The branching ratio is determined by the solvent dependent barrier heights $\Delta E_{[1,7]}$ and ΔE_{BHD}. Furthermore, it is instructive to consider the energetic differences between the CHT and its photoproducts compared to the perchlorinated case. As chlorine atoms are supposed to lower the energy of double bonds[53] (see also Figure 9), the differences in $CHTCl_8$ are smaller. Finally, the solvent dependence of the $BHDCl_8$ formation can be explained by the barrier height in the excited state, which obviously favors this competition reaction in unpolar solvents.

4. Conclusion and Outlook

In conclusion, the results can be interpreted as follows: After excitation with an ultrashort laser pulse at 263 nm to the 1A″ state, $CHTCl_8$ relaxes back to the ground state via two conical intersections (2A′−1A″, 1A′−2A′). At the 1A′−2A′ intersection, a photochemically allowed [1,7]-chlorine migration takes place. The mechanism is similar to the [1,7]-hydrogen migration in CHT. However, during the migration step the chlorine atom is partly negatively charged, which leads to a solvent-dependent relaxation time constant during the 1A′−2A′ intersection. In

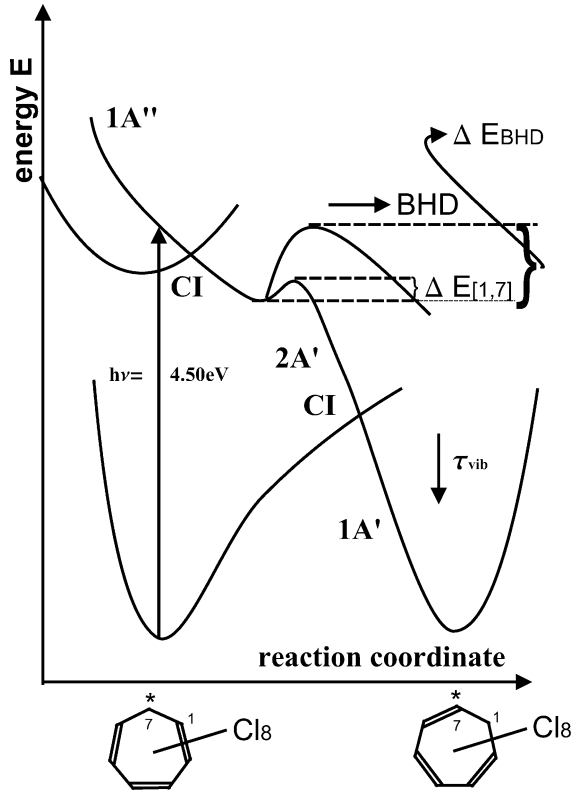

Figure 10. Sketch of the potential energy surface of $CHTCl_8$, adopted and modified from refs 26 and 28. After photoexcitation, the molecule reaches the 1A″ state and relaxes to the 2A′ state via a conical intersection. In the 2A′ state, the potential barriers, $\Delta E_{[1,7]}$ and ΔE_{BHD}, for the [1,7]-chlorine shift and the formation of BHD determine the branching ratio. In the case of the [1,7]-shift, the reaction reaches the ground state via a second conical intersection. Note that the 2D-plot is an oversiplification. In fact, conical intersections are supposed to be $3N - 8$ dimensional seams; therefore, the calculated energy for the [1,7]-transition is not necessarily identical with the energy of the molecule at the second conical intersection.

addition, a [4,5]-electrocyclization to $BHDCl_8$ takes place, but it does not play any role in femtosecond experiments because it is considerably slower. Solvent-independent fast anisotropy decays indicate vibrational motions of $CHTCl_8$ in the excited state. The investigation of $CHTCl_8$ also allows for an explanation of the high initial anisotropy and the complementary decay in CHT.

Nevertheless, there is need for further investigations in this field. Similar effects as in $CHTCl_8$ should be observable in systems like $CHTF_8$ and $CHTBr_8$ and even in perhalogenated cyclopentadienes, which might undergo a [1,3]-halogen shift, but not in permethylated $CHTMe_8$, where no charge separation is expected. Furthermore, an analysis of the vibrational relaxation in various solvents is important. For this, tuning of the probe and also the pump wavelengths is required. These measurements are also required to show the wavelength-independency of the first two time constants. Also, direct excitation of the dark state, 2A′, via a two-photon absorption may further enlighten the underlying electronic properties. For CHT, this state peaks at 284 nm (4.56 eV) as determined by magnetic circular dichroism studies.[79] According to theory[61] one would expect an anomalous high initial anisotropy (i.e., $0.57 \leq r_0 \leq 0.79$) in a two-photon-pump one-photon-probe experiment since the same degeneracy of the excited states is probed.

Acknowledgment. This work has been supported by the Deutsche Forschungsgemeinschaft, the Fonds der chemischen Industrie, and the Dr.-Otto-Röhm-Gedächtnisstiftung. Moreover, we thank Prof. H. Hippler for generous support of this work and Dr. A. Rapp and K. Imhof for the synthesis of $CHTCl_8$ as well as T. Bentz for technical assistance during manuscript preparation.

A. Appendix

A.1. IR Data of $CHTCl_8$. The IR spectrum of $CHTCl_8$ is shown in Figure 1 and the calculated vibrational frequencies using DFT calculation (B3-LYP/TZVP) are given in Table 1. Note that these frequencies are listed as received, i.e., without correction factor. For comparison, the experimental data are also inserted. The difference between experiment and theory does not exceed 5%.

A.2. Notes on the Dipole Moment of 2,2,2-Trichloroethanol (TCE). In this appendix, the dipole moment of TCE shall be briefly discussed, since its value is known to be 2.04 D[80] and therefore less than the value given in Table 2. However, there are two possible isomers, *cis*- and *trans*-TCE, where the cis isomer is energetically more stable ($\Delta E = 11.5$ kJ/mol using DFT (B3-LYP/TZVP)). The corresponding dipole moments have been determined to 1.43 D for the cis and 3.10 D for the trans isomer. Experiments to determine the dipole moment have been performed in benzene as solvent where a considerable amount of TCE is supposed to be in the thermodynamically more favorable cis isomer.[80] In pure TCE however, the trans isomer should be preferred as shown for ethanol and 2,2,2-trifluoroethanol,[81] leading to a larger effective dipole moment. Moreover a value of 3.4 D is given for the solid phase[82] which is close to the calculated value of 3.10 D for the trans-isomer. However, one should be aware of the fact that the calculations represent values for isolated molecules in the gas phase, whereas the condensed phase may lead to substantial shifts.

References and Notes

(1) Klessinger, M.; Michl, J., Ed. *Excited States and Photo-Chemistry of Organic Molecules*; VCH: New York, 1995.
(2) Fuβ, W.; Haas, Y.; Zilberg, S. *Chem. Phys.* **2000**, *259*, 273.
(3) Merer, A. J.; Mulliken, R. S. *Chem. Rev.* **1969**, *69*, 639.
(4) Hudson, B. S.; Kohler, B. E.; Schulten, S. *Excited States* **1982**, *6*, 1.
(5) Pullen, S. H.; Anderson, N. A.; Walker, N. A.; Sension, R. J. *J. Chem. Phys.* **1997**, *107*, 4985.
(6) Anderson, N. A.; Pullen, S. H.; Walker, L. A., II; Shiang, J. J.; Sension, R. J. *J. Phys. Chem. A* **1998**, *102*, 10588.
(7) Ohta, K.; Naitoh, Y.; Tominaga, K.; Hirota, N.; Yoshihara, K. *J. Phys. Chem. A* **1998**, *102*, 35.
(8) Lochbrunner, S.; Fuss, W.; Schmid, W. E.; Kompa, K. L. *J. Phys. Chem. A* **1998**, *102*, 9334.
(9) Fuss, W.; Schmid, W. E.; Trushin, S. A. *Chem. Phys.* **2005**, *316*, 225.
(10) Cardoza, J. D.; Dudek, R. C.; Mawhorter, R. J.; Weber, P. M. *Chem. Phys.* **2004**, *299*, 307.
(11) Cook, B. H. O.; Leigh, W. J. In *Chemistry of Dienes and Polyenes*; Rappoport, Z., Ed.; Wiley: Chichester, U.K., 2000; p 197.
(12) Assenmacher, F.; Gutmann, M.; Hohlneicher, G.; Stert, V.; Radloff, W. *Phys. Chem. Chem. Phys.* **2001**, *3*, 2981.
(13) Harris, D. A.; Orozco, M. B.; Sension, R. J. *J. Phys. Chem. A* **2006**, *110*, 9325.
(14) Fuss, W.; Panjy, S.; Schmid, W. E.; Trushin, S. A. *Mol. Phys.* **2006**, *104*, 1133.
(15) Krawczyk, R. P.; Malsch, K.; Hohlneicher, G.; Gillen, R. C.; Domcke, W. *Chem. Phys. Lett.* **2000**, *320*, 535.
(16) Ruiz, D. S.; Cembran, A.; Garavelli, M.; Olivucci, M.; Fuss, W. *Photochem. Photobiol.* **2002**, *76*, 622.
(17) Quenneville, J.; Martinez, T. J. *J. Chem. Phys.* **2003**, *107*, 829.
(18) Domcke, W; Yarkony, D.; Köppel, H. *Conical Intersections: Electronic Structure, Dynamics and Spectroscopy*; World Scientific: Singapore, 2004.
(19) Tamura, H.; Nanbu, S.; Ishida, T.; Nakamura, H. *J. Chem. Phys.* **2006**, *124*, 084313/1.

(20) Borell, P. M.; Löhmannsröben, H.-G.; Luther, K. *Chem. Phys. Lett.* **1987**, *136*, 371.
(21) Trushin, S. A.; Diemer, S.; Fuss, W.; Kompa, K. L.; Schmid, W. E. *Phys. Chem. Chem. Phys.* **1999**, *1*, 1431.
(22) Reid, P. J.; Wickham, S. D.; Mathies, R. A. *J. Phys. Chem.* **1992**, *96*, 5720.
(23) Reid, P. J.; Shreve, A. P.; Mathies, R. A. *J. Phys. Chem.* **1993**, *97*, 12691.
(24) Hertwig, A.; Hippler, H.; Schmid, H.; Unterreiner, A. N. *Phys. Chem. Chem. Phys.* **1999**, *1*, 5129.
(25) Ruan, C.-Y.; Lobastov, V. A.; Srinivasan, R.; Goodson, B. M.; Ihee, H.; Zewail, A. H. *PNAS* **2001**, *98*, 7117.
(26) Steuhl, H.-M.; Bornemann, C.; Klessinger, M. *Chem.—Eur. J.* **1999**, *5*, 2404.
(27) Bornemann, C.; Klessinger, M. *Org. Lett.* **1999**, *1*, 1889.
(28) Hippler, H.; Olzmann, M.; Schalk, O.; Unterreiner, A.-N. *Z. Phys. Chem.* **2005**, *219*, 389.
(29) Srinivasan, R. *J. Am. Soc. Chem.* **1962**, *84*, 3432.
(30) Trush, B. A.; Zwolenik, J. *J. Bull. Soc. Chim. Belg.* **1962**, *71*, 642.
(31) Dauben, W. G.; Cargill, L. R. *Tetrahedron* **1961**, *12*, 186.
(32) Samuni, U.; Kahana, S.; Haas, Y. *J. Phys. Chem. A* **1998**, *102*, 4758.
(33) Daino, Y.; Hagiwara, S.; Hakushi, T.; Inoue, Y.; Tai, *Am. J. Chem. Soc. Perkin Trans. II* **1989**, 275.
(34) Ter Borg, A. P.; Kloosterziel, H. *Recl. Trav. Chim. Pays-Bas* **1965**, *84*, 241.
(35) Ter Borg, A. P.; Kloosterziel, H. *Recl. Trav. Chim. Pays-Bas* **1969**, *89*, 266.
(36) Chung, G. Y.; Carr, R. W. *J. Chem. Phys.* **1987**, *91*, 2831.
(37) Hippler, H.; Luther, K.; Walsh, R. *J. Chem. Phys.* **1978**, *68*, 323.
(38) Looker, J. J. *J. Org. Chem.* **1972**, *37*, 1059.
(39) van Eis, M. J.; van der Linde, B. S. E.; de Kanter, F. J. J.; de Wolf, W. H.; Bickelhaupt, F. *J. Org. Chem.* **2000**, *65* 4348.
(40) Feigel, M.; Kessler, H. *Tetrahedron* **1976**, *32*, 1575.
(41) Töke, L.; Bende, Z.; Bitter, I.; Tóth, G.; Simon, P.; Soós, R. *Tetrahedron* **1984**, *40*, 4507.
(42) Koch, R.; Wong, M. W.; Wentrup, C. *J. Org. Chem.* **1996**, *61*, 6809.
(43) Okajima, T.; Imafuku, K. *J. Org. Chem.* **2002**, *67*, 625.
(44) Woodward, R. B.; Hoffmann, R. *Angew. Chem., Int. Ed. Engl.* **1969**, *8*, 781.
(45) Kusada, K.; West, R. *J. Am. Chem. Soc.* **1968**, *90*, 7354.
(46) Ahlrichs, R.; Bär, M.; Häser, M.; Horn, H.; Kölmel, C. *Chem. Phys. Lett.* **1989**, *162*, 165.
(47) Treutler, O.; Ahlrichs, R. *J. Chem. Phys.* **1995**, *102*, 346.
(48) Eichkorn, K.; Weigend, F.; Ahlrichs, R.; Treutler, O. *Theo. Chem. Act.* **1997**, *97*, 119.
(49) Lenzner, M.; Spielmann, C.; Winter, E.; Krausz, F.; Schmidt, A. *J. Opt. Lett.* **1995**, *20*, 1397.
(50) Sartania, S.; Cheng, Z.; Lenzner, M.; Tempea, G.; Spielmann, C.; Krausz, F.; Ferencz, K. *Opt. Lett.* **1997**, *22*, 1562.
(51) Zuccarello, F.; Buemi, G.; Raudino, A. *J. Comput. Chem.* **1980**, *4*, 341.
(52) Frueholz, R. P.; Rianda, R.; Kuppermann, A. *Chem. Phys. Lett.* **1978**, *55*, 88.
(53) Mingos, D. M. P. *Essential Trends in Inorganic Chemistry*; Oxford University Press: Oxford, U.K., 1998.
(54) Kusuda, K.; West, R.; Rao, V. N. M. *J. Am. Soc. Chem.* **1971**, *93*, 3627.
(55) *UV Atlas of Organic Compounds*; Oxford University Press: Oxford, U.K., 1966; Vol. 4.
(56) Two things are worth pointing out: First, the time scale for vibrational relaxation in TCE is comparable to other solvents although one could expect a more efficient energy transfer between $CHTCl_8$ and TCE due to similar vibrational frequencies. Second, the time constant for the vibrational relaxation is at least a factor of 3 larger than for CHT when pumped and probed at the same wavelengths.[24] This may be due to a higher excess energy of $CHTCl_8$ after pumping at 263 nm. Moreover, the IR frequencies in $CHTCl_8$ (see Table 1 in the appendix) are redshifted compared to CHT due to the Cl-mass effect. This leads to slower coupling between the vibrational modes and the solvent. Therefore, when calculating the vibrational temperature of CHT and $CHTCl_8$ assuming that the energy is deposited among the vibrational modes via a Boltzmann distribution, one finds 2200 K for CHT and 1600 K for $CHTCl_8$.
(57) The combined time constant for the perchlorined species can be obtained by deconvolution of the data with the time resolution of the experiment and refolding it with a pulse longer than the first time constant. If this is done, the combined time constant of $\sim$ 720 fs can be obtained. This time constant varies hardly when changing the length of the refolding pulse between 200 and 400 fs.
(58) Fleming, G. R. *Chemical Applications of Ultrafast Spectroscopy*, Oxford Univ. Press: Oxford, 1986.
(59) Cross, A. J.; Fleming, G. R. *Biophys. J.* **1984**, *46*, 45.
(60) Kawski, A. *Crit. Rev. Anal. Chem.* **1993**, *23*, 459.
(61) Schalk, O.; Unterreiner, A.-N. To be submitted to *J. Chem. Phys.*
(62) Wynne, K.; Hochstrasser, R. M. *Chem. Phys.* **1993**, *171*, 179.
(63) Knox, R. S.; Gilmore, R. C. *J. Lumin.* **1995**, *63*, 163.
(64) Razi Naqvi, K.; Dale, R. E. *Chem. Phys. Lett.* **2002**, *357*, 147.
(65) Galli, C.; Wynne, K.; Le Cours, S. M.; Therien, M. J.; Hochstrasser, R. M. *Chem. Phys. Lett.* **1993**, *206*, 493.
(66) Hrong, M. L.; Gardecki, J. A.; Papazyan, A.; Maroncelli, M. *J. Phys. Chem.* **1995**, *99*, 17311.
(67) Marcus, R. A. *Rev. Mod. Phys.* **1993**, *65*, 599.
(68) Levine, R. D. *Molecular Reaction Dynamics*; Cambridge University Press: Cambridge, U.K., 2005.
(69) Scheiner, S. *J. Phys. Chem. A* **2000**, *104*, 5898.
(70) Chou, P.-T.; Yu, W.-S.; Cheng, Y.-M.; Pu, S.-C.; Yu, Y.-C.; Lin, Y.-C.; Huang, C.-H.; Chen, C.-T. *J. Phys. Chem. A* **2004**, *108*, 6487.
(71) Böttcher, C. F. J. *Theory of Dielectric Polarization*; Elsevier: Amsterdam, 1973.
(72) Fuss, W.; Schmid, W. E.; Trushin, S. A. *J. Am. Chem. Soc.* **2001**, *123*, 7101.
(73) Fuss, W.; Pushpa, S.; Schmid, W. E.; Trushin, S. A. *J. Phys. Chem. A* **2001**, *105*, 10640.
(74) Lochbrunner, S.; Zissler, M.; Piel, J.; Riedle, E.; Spiegel, A.; Bach, T. *J. Chem. Phys.* **2004**, *120*, 11634.
(75) Note that there remains an uncertainty, since it still has to be shown, that the time constants are independent of the wavelength. It might be the case that the second time constant arises from another relaxation process that does not involve a simple state-to-state transition. However, both DFT calculations and a comparison with CHT support an interpretation as outlined.
(76) Hawkes, G. E.; Smith, R. A.; Roberts, J. D. *J. Org. Chem.* **1974**, *39*, 1276.
(77) Roedig, A.; Hörnig, L. *Ann. Chem.* **1956**, *598*, 208.
(78) Abraham, M.; Kharlanov, V. In *Handbook of Photochemistry and Photobiology*; Nalwa, H. S., Ed.; American Scientific Publishers, 2003; Vol. 2, p 299.
(79) Dauben, W. G.; Seeman, J. I.; Wendschuh, P. H.; Barth, G.; Bunnenberg, E.; Djerassi, C. *J. Org. Chem.* **1972**, *37*, 1209.
(80) Krishnamurthy, S. S.; Soundararajan, S. *J. Chem. Phys.* **1969**, *73*, 4036.
(81) Radnai, T.; Ishiguro, S.; Otaki, H. *J. Solution Chem.* **1989**, *18*, 71.
(82) Lopez, D. O.; Tamarit, J. L.; de la Fuente, M. R.; Pérez-Jubindo, M. A.; Salud, J.; Barrio, M. *J. Phys.: Condens. Matter* **2000**, *12*, 3871.
(83) Bartoli, F. J.; Litovitz, T. A. *J. Chem. Phys.* **1972**, *56*, 413.
(84) Arnett, D. C.; Vöhringer, P.; Scherer, N. F. *J. Am. Chem. Soc.* **1995**, *117*, 12262.